

Application of Electrochemical Impedance Spectroscopy (EIS) to Study the Effect of Temperature and Ion Concentration During Electroplating of Copper from an Acidic Bath

Sudeshna Parida¹  · Sanjeev Das² · Archana Mallik¹

Received: 30 April 2023 / Accepted: 9 November 2023 / Published online: 20 December 2023
© The Indian Institute of Metals - IIM 2023

Abstract In the present investigation, copper electrodeposition from an acidic bath at low temperature and varying copper ion concentrations has been studied by using electrochemical impedance spectroscopy (EIS). A fitted equivalent circuit was utilized to determine EIS parameters. Double-layer capacitance (C_{dl}) values for 0.1 M and 0.5 M Cu concentrations are 90 and 82 μF , whereas Gouy–Chapman capacitance (C_{diff}) at constant potential values is 55 and 122 μF . The C_{dl} values ranged from 44 to 87 μF as the temperature increased from 5 to 25 °C, while the C_{diff} values extended from 112.76, 105.4, 98.66, 92.53 and 86.96 μF . It was found that the diffusion coefficient (D) values increased with temperature and low molar concentration of Cu. The value of electrochemical activation energy was obtained to be 35.19 kJ/mol. The obtained copper deposits were studied by atomic force microscopy (AFM) and scanning electron microscope (SEM). It was observed that the deposits were denser and adherent at low temperatures and all concentrations.

Keywords Copper · Electro-crystallization · EIS · Temperature · Diffusion coefficient

1 Introduction

Electro-crystallization of metal on different surfaces still gets a lot of attention in modern electrochemistry because of the versatility of the technology for fabricating components for different high-end applications. During electroplating, current density and electrode potential can be used to manipulate the driving force of the electrodeposition process [1]. However, temperature can play a crucial role in the nucleation and growth mechanisms, as it can strongly influence the structure and shape of metal deposits [2]. Moreover, low temperature has a significant role in electrochemical systems where interdiffusion of deposits can arise. In an electrochemical system, the metal ions are deposited onto the substrate surface during the period of bias application and generate adatoms that diffuse over the substrate; these adatoms finally interact with other adatoms. Finally, the establishment of atomic clusters occurs on the substrate surface which remains stable or unstable. Unstable clusters disappear over time, but stable clusters get able to expand and finally create a film or deposit. However, at low temperatures, the deposition mechanism might have typical characteristics, i.e., low diffusion coefficient and low deposition rate. From a thermodynamic point of view, the barrier energy that metal ions must overcome to form an adatom is dependent on temperature [3]. Meanwhile, low-temperature electrodeposition has 2 perspectives: a fall in the thermodynamic barrier and a rise in the kinetic barrier. At a constant concentration in the nucleation model, the nucleation rate J is dependent on the process's limits according to the following equation [4]

$$\ln J = K_1 - 2\theta\sigma^3 v^2 / [k_B T (\text{ne})^2 \eta_n^2] \quad (1)$$

✉ Sudeshna Parida
sudeshnaparida897@gmail.com

¹ Electrometallurgy and Corrosion Laboratory, Department of Metallurgical and Materials Engineering, NIT Rourkela, Rourkela 769008, India

² Advanced Metal Casting Laboratory, Department of Metallurgical and Materials Engineering, NIT Raipur, Raipur, Chhattisgarh 492010, India

where η_n is the nucleation overpotential, θ is the interface of metal crystal and substrate (shape factor), K_1 is dependent on exchange current density, where σ is the specific surface energy at the metal–electrolyte interface, v is the volume per atom, ne is the charge transferred when one atom is linked to a cluster, and k_b and T have their usual meaning.

There are several investigations on the electrochemical crystallization of copper at low temperatures using different microscopic techniques [3, 5]. Several copper deposition mechanisms are proposed by authors at room temperature and different ion concentrations [6–10]. Grujicic et al. reported that as copper concentration increased, nuclei size grew, while nuclei density decreased [7]. However, no mechanism investigates the effect of concentration in the EIS method. Some authors have also reported only the electrodeposition characteristics of copper, nickel, and silver at low temperatures [5, 11, 12]. Some authors have discussed the deposition of metals at room temperature by using EIS [13–16]. However, there are very few investigations on the use of EIS to study the effect of temperature and ion concentration on electroplating during deposition from acid solutions. So, in the present work, the main attention is to distinguish the kinetic of copper electrodeposition in an electrochemical system at low temperatures and various copper ion concentrations through EIS. Further, the quality of the thin film is studied by atomic force microscopy (AFM) along with scanning electron microscope (SEM) analysis.

2 Methodology

From an electrolyte of 0.25 M $\text{CuSO}_4 \cdot 5\text{H}_2\text{O}$ and 40 gL^{-1} H_2SO_4 , Cu was electroplated onto graphite electrodes (area of 0.25 cm^2). The pH of the solution was found to be 0.6

at the chosen concentration. The counter and reference electrodes are platinum, and saturated calomel electrode (SCE) respectively. Linear sweep voltammetry (LSV) was carried out at different temperatures (5, 10, 15, 20 °C and room temp) and copper ion concentration (0.1 and 0.5 M) at a scan rate of 0.1667 mV/s in the scan range of 0 V–1 V. The temperature of the depositing bath was 1st reduced in a chiller for the targeted value. Then after, during the synthesis the temperature was maintained by completely submerging the depositing bath in an ice-cooled and anti-freezer added water bath. The selected potential for electroplating from the LSV curve of each temperature was –260 mV/SCE. While electroplating, electrochemical impedance spectroscopy (EIS) was performed in frequency range of 10 mHz to 10 kHz and an amplitude of 10 mV. After the EIS study, AFM and SEM analysis were conducted.

3 Results

3.1 Assessment of Deposition Conditions

Figure 1a and b represents the relationship between current and potential at different copper ion concentrations (0.1, 0.25 and 0.5 M) and temperatures (5–25 °C). The relation between current and potential was measured from an initial potential of 0 V to a final potential of –1 V. Significant increase in current values was observed to be after a potential of –700 mV. However, the calculated equilibrium potentials for all the temperatures and concentrations were found to be in between –0.24 and –0.34 V. Hence, the potential of –0.26 V was chosen for experimentation as there has been no study reported for this potential.

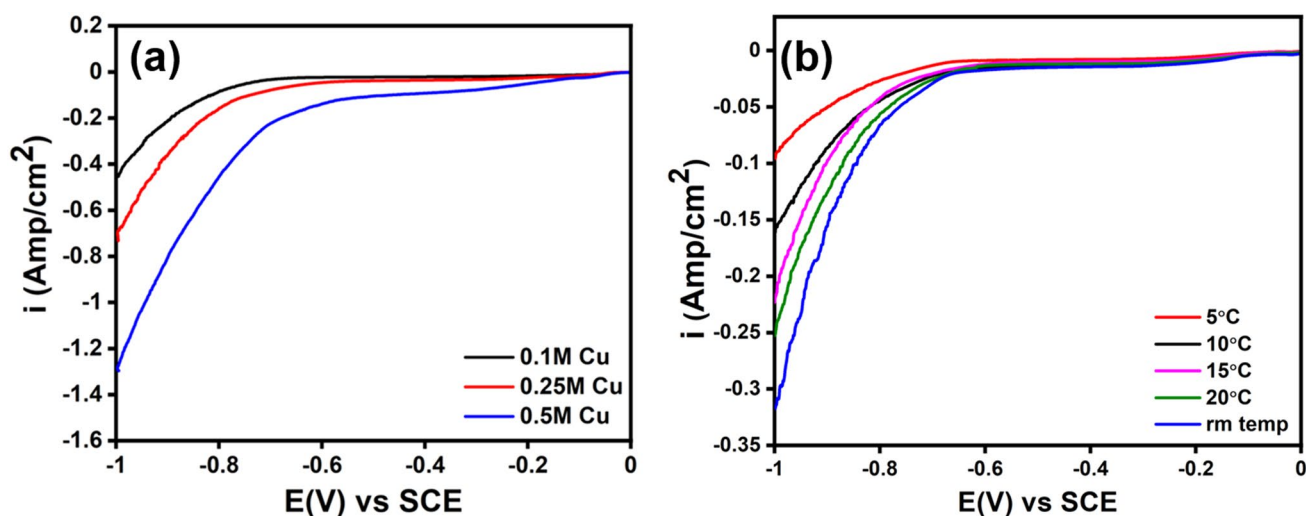


Fig. 1 a Current–potential curves in various Cu concentrations and b at different temperatures

Further the predominant ion concentration at the chosen temperature, composition, potential and pH was done through a thorough study by using FactSage 8.2. The phase diagram of the aqueous copper-sulfuric acid system is a useful tool for understanding the behavior of copper and sulfuric acid in water and predicting the conditions under which different phases of copper and sulfuric acid will coexist. Figure 2 shows the phase diagram of aqueous system $H_2O-H_2-H_2SO_4-CuSO_4$ at various ion concentrations and temperatures. The predominant phases are either aqueous or a precipitated one. In the Cu_2S + aqueous region and $CuSO_4(H_2O)5$ + aqueous region pH is varying differently in

both regions. The equilibrium system composition of Cu^+ and Cu^{2+} is given in Table 1 at the same pH and potential for different temperatures and ion concentrations.

3.2 Phase Formation Path and Mechanism

EIS studies were carried out to analyze the steps and detailed mechanism during electroplating of copper. The obtained spectra are fitted to equivalent circuit (EC) models to extract different parameters. The Nyquist plots and the Bode plots for varying deposition temperatures (5–25 °C) and concentrations are presented in Fig. 3. As

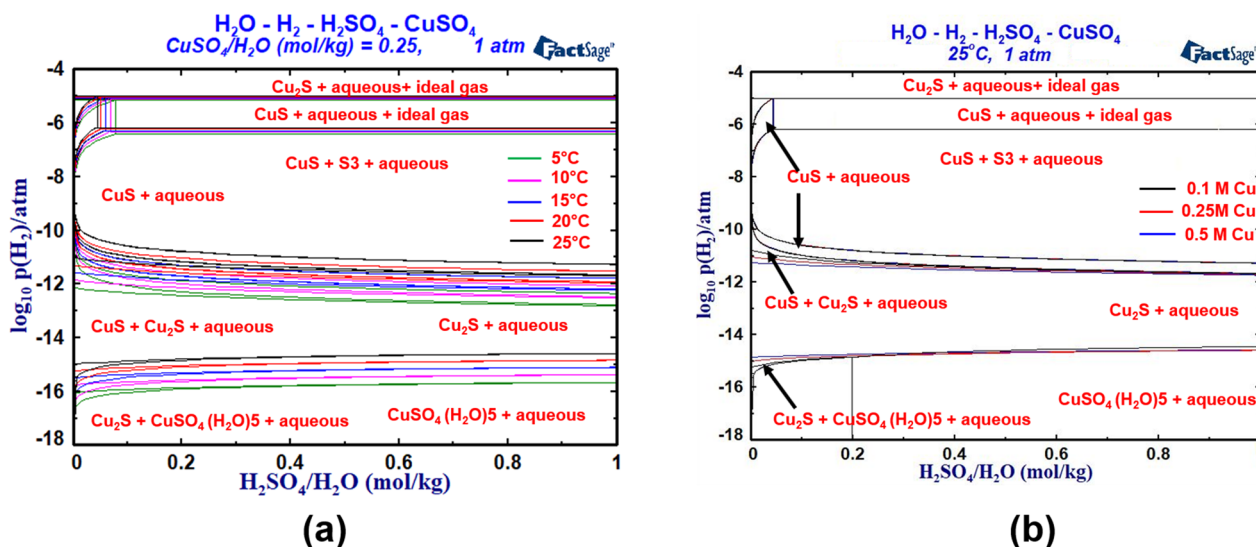


Fig. 2 Phase diagram of aqueous system $H_2O-H_2-H_2O-CuSO_4$ **a** different temperatures, **b** different concentrations

Table 1 Ion concentration at equilibrium state points of (a) Cu_2S phase and aqueous region, (b) $CuSO_4(H_2O)5$ phase and aqueous region, at different temperatures (5 to 25 °C), 1 atmospheric pressure and pH = 0.60

Parameters from FactSage	Molar concentration of copper ion in electrolyte						
	0.25 M					0.1 M	0.5 M
(a)	5 °C	10 °C	15 °C	20 °C	25 °C	25 °C	25 °C
H^+	0.25163	0.24880	0.24752	0.25103	0.24989	0.25092	0.25524
Cu^{2+}	2.3E-06	2.0E-05	5.8E-05	3.3E-05	3.2E-05	1.02E-05	1.04E-05
Cu^+	4.13E-10	3.58E-09	1.27E-08	1.16E-08	1.68E-08	6.69E-09	6.68E-09
E^h	0.35 V	0.36 V	0.36 V	0.35 V	0.35 V	0.35 V	0.35
Parameters from FactSage	Molar concentration of copper ion in electrolyte						
	0.25 M					0.1 M	0.5 M
(b)	5 °C	10 °C	15 °C	20 °C	25 °C	25 °C	25 °C
H^+	0.24881	0.25021	0.24590	0.25010	0.24846	0.24951	0.24585
Cu^{2+}	7.8E-02	8.9E-02	9.9E-02	0.11	0.12	9.8E-02	0.127
Cu^+	1.7E-07	2.8E-07	4.3E-07	6.8E-07	1.3E-06	1.4E-06	1.8E-06
E^h	0.45 V	0.45 V	0.46 V	0.46 V	0.45 V	0.45	0.45

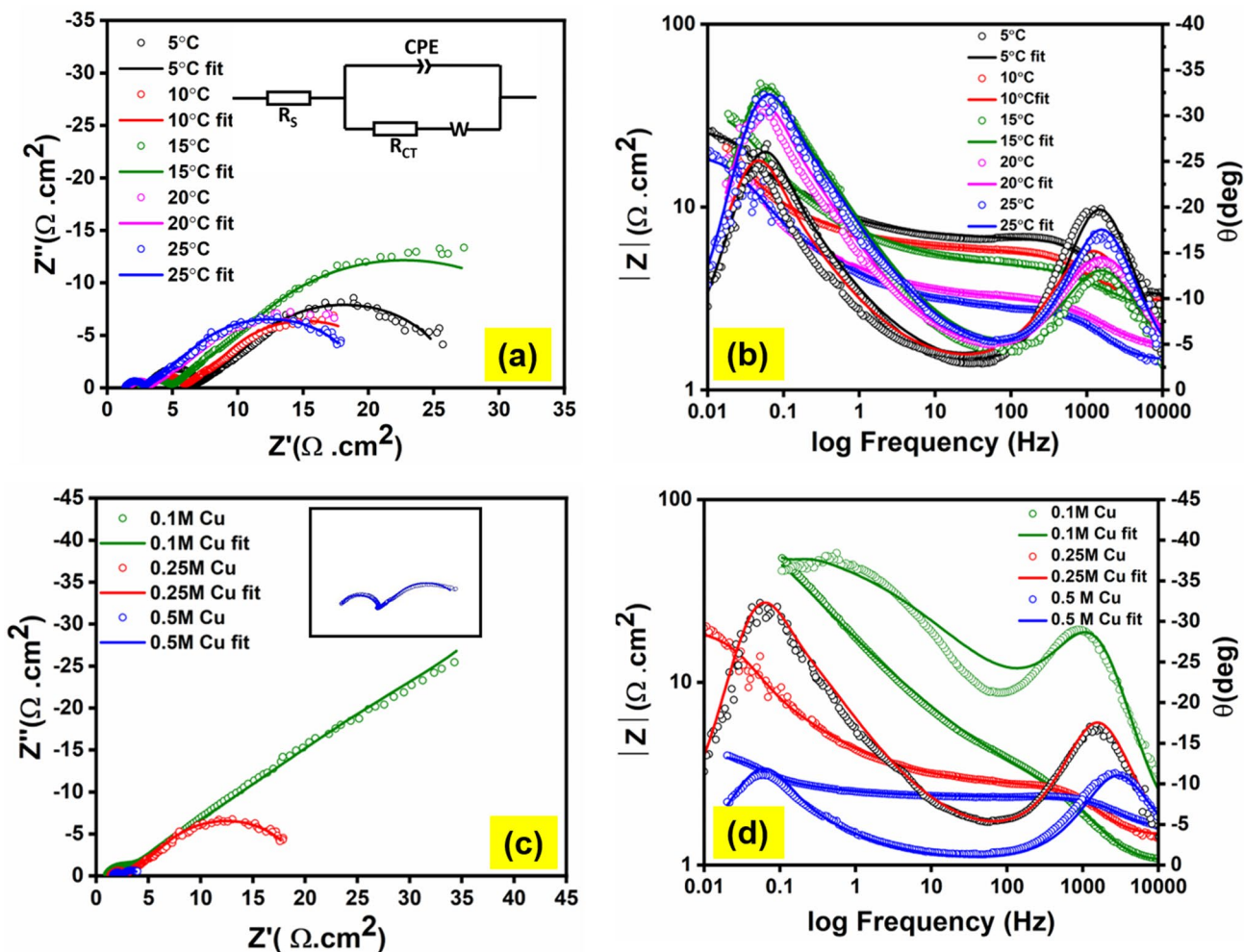


Fig. 3 Nyquist plots **a** at different temperatures, **c** different ion concentration, Bode plots **b** at different temperatures, **d** different ion concentrations during deposition of copper

shown in Fig. 3 (inscribed in Fig. 3a) for all temperatures (deposited at -0.26 V with 0.25 M ions) and ion concentrations, the EC model of the depositing system consists of a Randles circuit with a diffusion impedance. Hence, the model of the interface is composed of solution resistance (R_s), connected in series to a parallel circuit comprising of charge transfer resistance (R_{ct}), diffusion resistance (W , Warburg), and a constant phase element (CPE) corresponding to double-layer capacitance (C_{dl}). Generally, the impedances at low frequency correspond to diffusion contributions and surface concentration relaxation in adatoms, while high frequency corresponds to nucleation and growth as well as continuous film contribution. In the plots, 2 semicircles can be observed. The 1st semicircle (high frequency) corresponds to the capacitive nature of the electrochemical system, whereas the 2nd semicircle would correspond to the diffusion-dominated kinetics of the system at low frequency. The high and intermediate

frequencies would characterize the formation and growth of monolayers, which propagate over a finite distance and are dependent on the mode of deposition growth [17]. The diameters of both the semicircles are increasing as a function of lowering temperature and concentration. The inset in Fig. 3d indicates that at high molar concentrations of copper ions, charge transfer resistance decreases.

The contribution of each of the equivalent circuit parameters like R_s , R_{ct} , C_{dl} and W_s is discussed to estimate the effect of temperature and concentration. It can be observed there is variation of solution resistance values (R_s), i.e., increase with decrease in temperature and increase with increase in metal ion concentration. The increase of conductivity (or decrease of resistivity) with temperature is quite obvious as it will affect the mobility of the ions. Apart from temperature the dependency of conductivity of a solution on ion concentration can be defined as per Eqs. 2 and 3 provided below [18].

$$\text{Conductivity}(\Lambda) = \alpha(\tau^+\lambda^+ + \tau^-\lambda^-) \tag{2}$$

$$\lambda_i = \frac{Z_i F}{f(C_i)} \tag{3}$$

where α represents the degree of dissociation, τ^+ is the charge number of the cation, and λ^+ corresponds to the molar conductivity of the cation. Correspondingly, τ^- and λ^- represent the number of charges and molar conductivity of the anion. C_i is the species concentration, Z_i is the atomic number of the species, and F stands for the Faraday constant. It can be observed from Eq. 3 that increase in ionic concentration will decrease the ionic mobility, and hence the conductivity will decrease (or R_s will increase). Therefore, the fluctuation of R_s may be a result of variations in concentration. Now analyzing the double-layer capacitance values (C_{dl} , calculated using Brug’s relationship from the CPE, following Eq. 4), the value has been found to get increased with increase of temperature. There is a correlation between ion concentration and ion–ion interactions. If the concentration of ions increases, then the ion–ion interaction decreases which result in decreased ion mobility. A decrease in ion mobility can slow down the formation of a well-defined double layer and can restrict the amount of charge that can be stored. Accordingly, C_{dl} values are found to be decreased with increase of metal ion concentration in the bath. A lower C_{dl} indicates that fewer charges can be stored at the interface. In general, an increase in the C_{dl} would specify that the interface between the electrode and electrolyte has become more conductive and can store more charge. This can have significant implication for electrochemical processes that rely on the transfer of charge across the interface during electrodeposition. Understanding the changes in C_{dl} is thus a crucial aspect of the study of electrochemical systems. Guoy and Chapman have developed another theoretical description of the layers developed at the electrode/electrolyte interphase. In addition to C_{dl} , there can be a diffused portion of the double layer (C_{diff}). This model addresses ions as point charges, so that their motions in electrolytes are governed by diffusion. This ion transport determines the overall capacitance value which is significantly dependent on applied potential and the ion types in the electrolyte. Hence, attempt was made to check the applicability of Gouy–Chapman theory in the current study as given in Eq. 5 [19]:

$$C_{dl} = (\text{CPE}_T)^{\frac{1}{n}} \times \left(\frac{1}{R_S} + \frac{1}{R_{CT}} \right)^{\frac{n-1}{n}} \tag{4}$$

$$C_{diff} = \left(\frac{\epsilon e^2 C_0}{2\pi kT} \right)^{1/2} \cos h \frac{eE}{2kT} \tag{5}$$

where ϵ , e , E , k , and T have their usual meaning. According to Eq. (5) it can be found that diffusion capacitance (C_{diff}) is inversely proportional to the temperature. The calculated capacitance values are 112.76, 105.4, 98.66, 92.53, and 86.96 μF for depositions at 5, 10, 15, 20, and 25 °C, respectively. It is observed that C_{dl} values from Brug’s theory increases as temperature increases, whereas capacitance values from Gouy–Chapman’s theory decreases as temperature increases. Therefore, it can be assumed that the C_{dl} is not a diffused 3-layered structure but would be as of that Helmholtz layer capacitance. Now focusing on the charge transfer resistance values, R_{ct} has been found to be expressively increased from a value of 1.3 to 3.3 $\Omega \text{ cm}^2$ as temperature has dropped. For variation of metal ion concentration, the value has decreased from 1.37 to 0.78 $\Omega \text{ cm}^2$ as the molarity increases from 0.1 to 0.5. The value mainly depends on the ease of ionic charge transfer through the double layer and electronic charge transfer at the electrode. Accordingly, R_{ct} is inversely proportional to the double-layer capacitance as presented in Eq. 4.

Higher charge transfer resistance may indicate lower electron transfer. At lower temperature, higher R_{ct} would indicate lower electron transfer, complimenting further to the higher C_{diff} values and vice versa. Higher charge transfer resistance refers to more difficult for charged species (such as ions or electrons) to move across the interface between 2 phases, such as an electrode and an electrolyte. Hence, a slow kinetics can be expected with decreasing temperature.

For variation of metal ion concentration, the same framework of logic could not be put forward as the C_{dl} capacitance is invariant or decreasing marginally with metal ion concentration. Then, it must be the type and extent of diffusion which would control the kinetics. C_{diff} is inversely proportional to diffuse layer thickness. Due to diffuse layer compression, this increases Gouy–Chapman capacitance. Additionally, as concentrations increase, the mobility of ions decreases because there are more ions involved. The diffusion component at low frequencies may imply a mixed kinetics and hence has been analyzed critically here. The experimentally fit model for copper deposition accounts for the mass transport of dissolved species to and from the substrate via diffusion. In addition, the values of the diffusion coefficient vary from low molar concentration to high molar concentration in decreasing order. The diffusion rates are very slow at low temperatures; therefore, the diffusion coefficient values are low at low temperatures, which may further indicate a low kinetics. Further, the diffusion layer thickness was calculated by using Eq. (6) by substituting all the known parameters.

$$W_T = \frac{\delta^2}{D} \tag{6}$$

where W_T is the Warburg interpretation which is obtained from fitting the EIS curve, δ is the diffusion layer thickness, and D is the diffusion coefficient. The diffusion layer thickness increases as the temperature increases from 5 to 25 °C, while the ion concentration decreases, as shown in Table 2. Hence for temperature variation, the kinetics is expected to be a mixed kinetics as charge transfer resistance is increasing and diffusivity is decreasing with low temperature. Furthermore, the impedance is a short Warburg (W_s) for all conditions except the deposition at 0.1 M, i.e., the lowest metal ion concentration where an open Warburg (W_o) has been fitted. Short Warburg and open Warburg describe the impedance of a finite-length diffusion with transmissive and reflective boundary, respectively. Hence, ion concentration variation would be a diffusion-dominated kinetics as compared to temperature variation kinetics. Further, the Bode plots have been studied for more information as shown in Fig. 3b and d. All Bode plot signifies the same trend from 10,000 to 100 Hz in which a constant phase element (CPE) is present. In Fig. 3, the phase angle has shifted from -5 to -15° ; then, it becomes 0° where a charge transfer resistance is present. Again, from the Bode plot, it signifies the same trend from 100 to 0.01 Hz in which mass transfer occurs from electrode surface to electrolyte and the phase angle shifts from 0 to -30° and finally it decreases due to the presence of Warburg resistance.

At this juncture, it can be inferred that the rate of Cu^{2+} ion incorporation into the crystal is significantly contributed by both the rate of electron discharge and ionic diffusion which ultimately determines the growth rate. Hence, there are 2 processes involved: an electron transfer reaction with nucleation and growth, and a diffusion and charge transfer process combination during potentiostat study.

Further, the kinetics of the electroplating process is then analyzed through statistical mechanics. In the

electrochemical process, the rate constant (k_i) is explained and represented by the following expression

$$k_i = k_0 e^{\frac{-E_a}{RT}} \tag{7}$$

where k_0 is a constant known as the pre-exponential term and is generally dependent on the system behavior to the stimulus as well as T , T is the absolute temperature, E_a is the electro-chemical activation energy, and R is the gas constant. By using Eq. (7) the activation energy for the grain growth was calculated from the temperature range of 5–25 °C. Figure 4a shows the Arrhenius plot, and it confirms a linear relationship of rate constant with temperature. The activation energy for the diffusion of Cu ions [2] has been determined to be 50.63 kJ/mol. However, for our study activation energy is determined to be around 35.19 kJ/mol, which may indicate a mixed controlled kinetics, complimenting the EIS analysis.

Then the exchange current density values are determined by using Eq. (8) to further complement the observations in the previous sections.

$$i_0 = \frac{R_T}{nFR_{CT}} \tag{8}$$

where n is the number of electrons, T is the absolute temperature, F is the Faraday constant, R_{ct} is the charge transfer resistance, and R is the universal gas constant. It is found that by varying temperature from lower to higher the values themselves have increased as shown in Fig. 4b. It is also found that by varying ion concentration from lower to higher the values themselves have increased as shown in Fig. 4c. The rate of copper electrodeposition can be related to the exchange current density

$$k_i = i_0/nFAC \tag{9}$$

where k_i is the rate constant n , F , C and A have their usual meaning. Combining Eqs. (8) and (9), we get

Table 2 Fitted EIS parameters during electroplating of copper at different temperatures and ion concentrations

EIS parameters	Temperature (°C)					Ion concentration (M)	
	5	10	15	20	25	0.1	0.5
R_s ($\Omega \text{ cm}^2$)	3.28	2.967	2.766	1.676	1.384	1.039	1.577
CPE_p (n)	0.99	0.86	0.90	0.86	0.88	0.99	0.97
R_{ct} ($\Omega \text{ cm}^2$)	3.3	2.7	1.8	1.4	1.3	1.374	0.78
C_{dl} (μF)	44.06	60.67	62.66	84.62	87.28	90.75	82.46
$W-R$ ($\Omega \text{ cm}^2$)	19.84	16.23	31.22	16.83	16.95	119.4	1.667
$W-T$	12.66	15.52	15.15	15.68	14.95	14.46	8.147
D (cm^2/s) $\times 10^{-6}$	0.17	0.22	0.33	0.8	1.88	1.70	4.22
δ (μm)	14.6	18.5	22.5	35.5	53	49.58	58.63
i_0 (mA/cm^2)	3.6	4.5	6.8	9.0	9.8	9.3	16

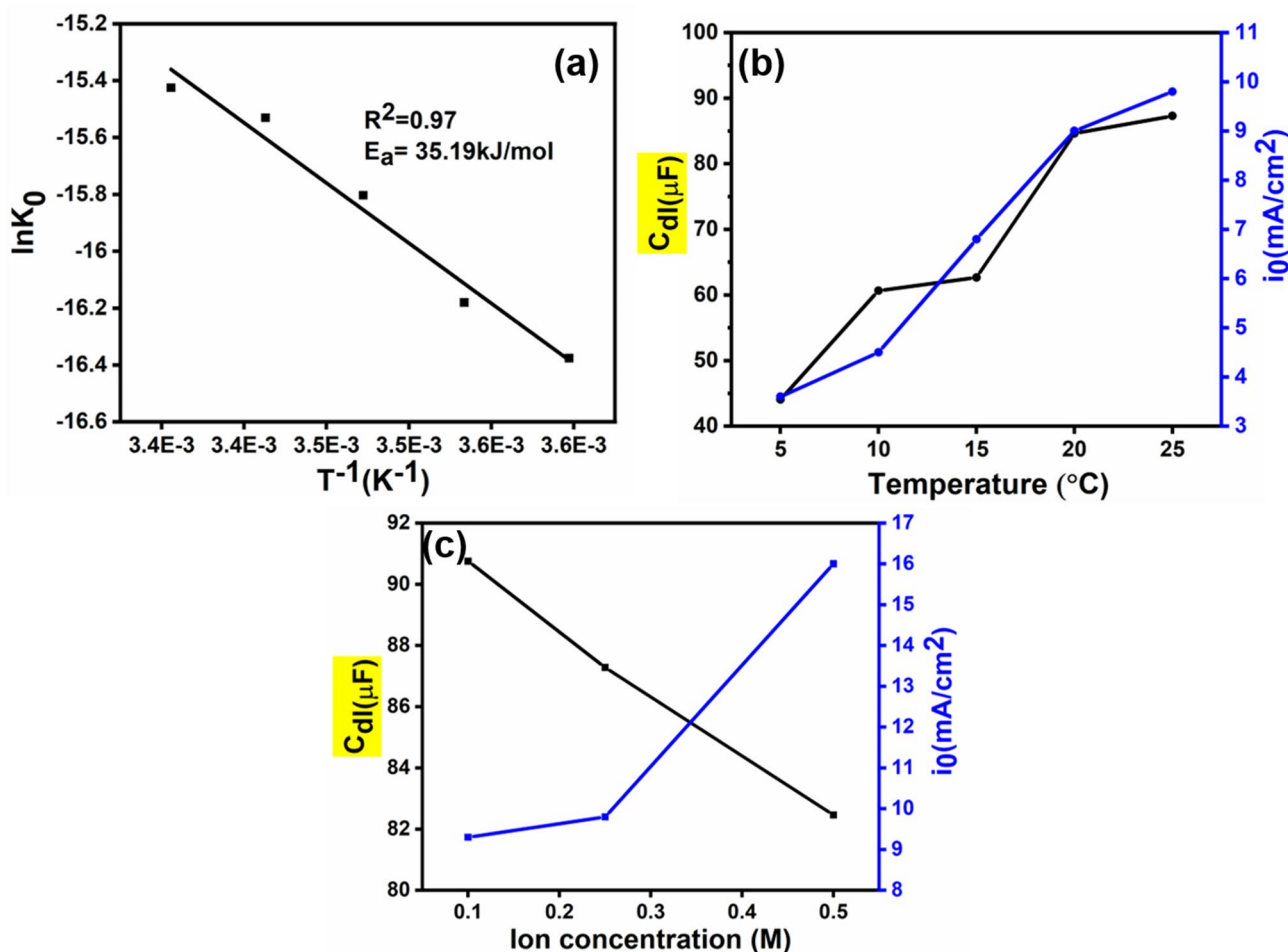


Fig. 4 a Arrhenius plot b and c relation between double-layer capacitance and exchange current density during electroplating of copper with different temperatures and ion concentrations

$$i_0 = k_0 e^{\frac{-E_a}{R_T}} n F A C \tag{10}$$

From Eq. (10) it can be found that exchange current density is exponentially related to the activation energy. Again, the relationship between rate constant and charge transfer resistance is expressed as follows

$$k_i = R_T / n^2 F^2 R_{CT} A C \tag{11}$$

Putting Eq. (10) into Eq. (8), then we get

$$R_T / n^2 F^2 R_{CT} A C = k_0 e^{\frac{-E_a}{R_T}} \tag{12}$$

Let us assume $S_0 = R_T / n^2 F^2 R_{CT} A C$ then Eq. (12) becomes

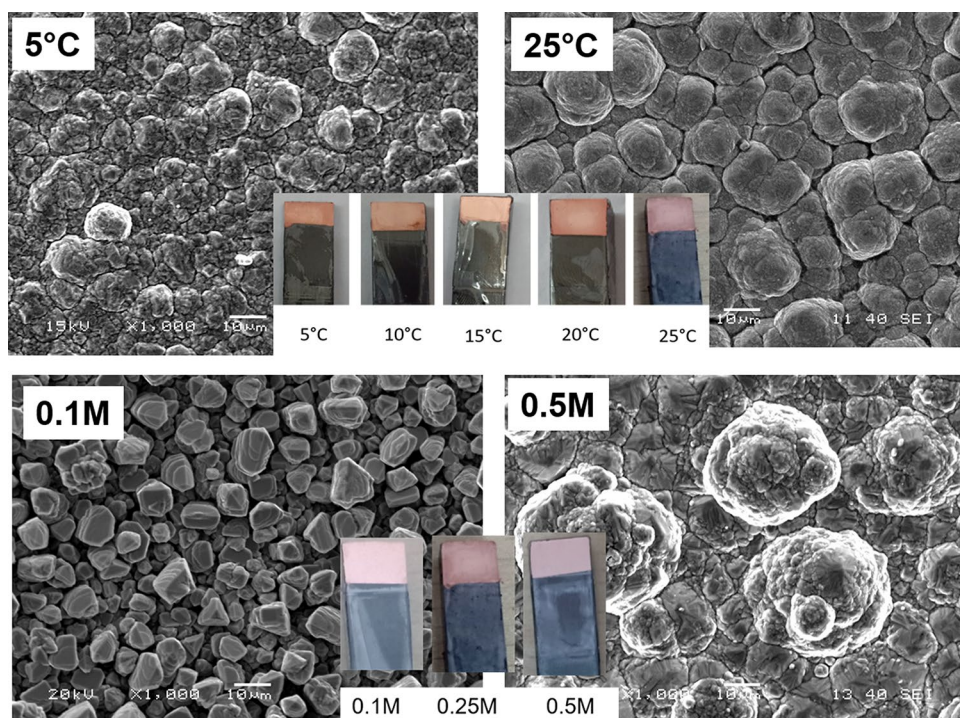
$$k_0 = S_0 / e^{\frac{-E_a}{R_T}} \tag{13}$$

where K_0 is the pre-exponential factor which is determined by Eq. (13). So, it has been found that the pre-exponential factor (K_0) is inversely proportional to the charge transfer resistance.

3.3 Structural Study of Electroplated Copper Films

Figure 5 shows the SEM micrographs for copper films deposited at 5 and 25 °C (at concentrations of 0.25 M), 0.1 M (25 °C), and 0.5 (25 °C). As there is no change in grain architecture, the micrographs of only high and low temperature have been presented here. It can be observed that deposits are compact and quite adherent to the substrate as the temperature is decreasing and concentration is increasing. The structural properties are further explored with AFM as shown in Fig. 6. The average roughness (Ra) of deposits at 0.1 M and 0.5 M Cu concentrations is 87.6 and 138 nm, respectively. For temperature variations, Ra values vary from 163 to 258 nm as temperature is varied from 5 to

Fig. 5 SEM micrographs for copper films deposited at 5 and 25 °C (at concentrations of 0.25 M), 0.1 M (25 °C), and 0.5 (25 °C)



25 °C. It can be argued that due to the low growth rate, the lowest roughness is attained at 5 °C. At higher temperatures and ion concentrations more energy should be available for the atoms to acquire so that they can diffuse and occupy the proper position within the crystal lattice, and grains with lower surface energy will expand at higher temperatures (room temperature). This would lead to a rougher deposit. The root-mean-square roughness (R_q), which is the square root of the surface height distribution, is more sensitive to measurement than Ra. The nanoscope analysis reveals 204, 282, 255, 275, and 313 nm at various temperatures and 114 and 176 nm for 0.1 M and 0.5 M copper ion concentration, respectively. It is also very evident that as the ion concentration rises, the number of grains decreases. It is also possible to conclude that the number of grain boundaries increases as temperature and ion concentrations decrease. At low temperatures, the number of nuclei is expected to be more because of supersaturation effect and hence nucleation population density would be also high.

4 Conclusion

In the present investigation, EIS has been used extensively to analyze the effect of ion concentration and temperature on copper electroplating and the salient results are summarized below.

- It was found that all the EIS spectra obtained for all the ion concentration and temperatures at constant potential had general trend, consisting of charge transfer as well as diffusion-controlled impedances, i.e., a mixed kinetics could be expected.
- It was found that C_{dl} values ranged from 44.06, 60.67, 62.66, 84.62, to 87.28 μF for depositions at 5, 10, 15, 20, and 25 °C, respectively, and 90.75, 87.28, and 82.46 μF for depositions at 0.1, 0.25, and 0.5 M, respectively. The R_{ct} values 1.3, 1.4, 1.8, 2.7, and 3.3 Ω with decrease of temperature and 1.37, 1.3 0.78 Ω with increase of ion concentration. Hence, the mixed kinetics would have a dominance of charge transfer at low temperature. However, the diffusivity also decreased with temperature reduction; hence, the kinetics was always a mixed one for all temperatures at the chosen potential. For variation of metal ion concentration, the kinetics was found to be dominated by the diffusivity.
- The above observation was further complimented by the calculated electrochemical activation energy value which was found to be 35.19 J/mol, indicating a mixed kinetics. Further, the exchange current density was increasing with increase of both the parameters.
- The obtained copper deposits were found to be uniform and adherent when the kinetics was mixed controlled (for all temperatures) and at all ion concentrations. The observation that 0.1 M Cu deposits appeared powdery and smooth, while 0.5 M Cu deposits appeared compact and rough, suggesting diffusion-dominated kinetics.

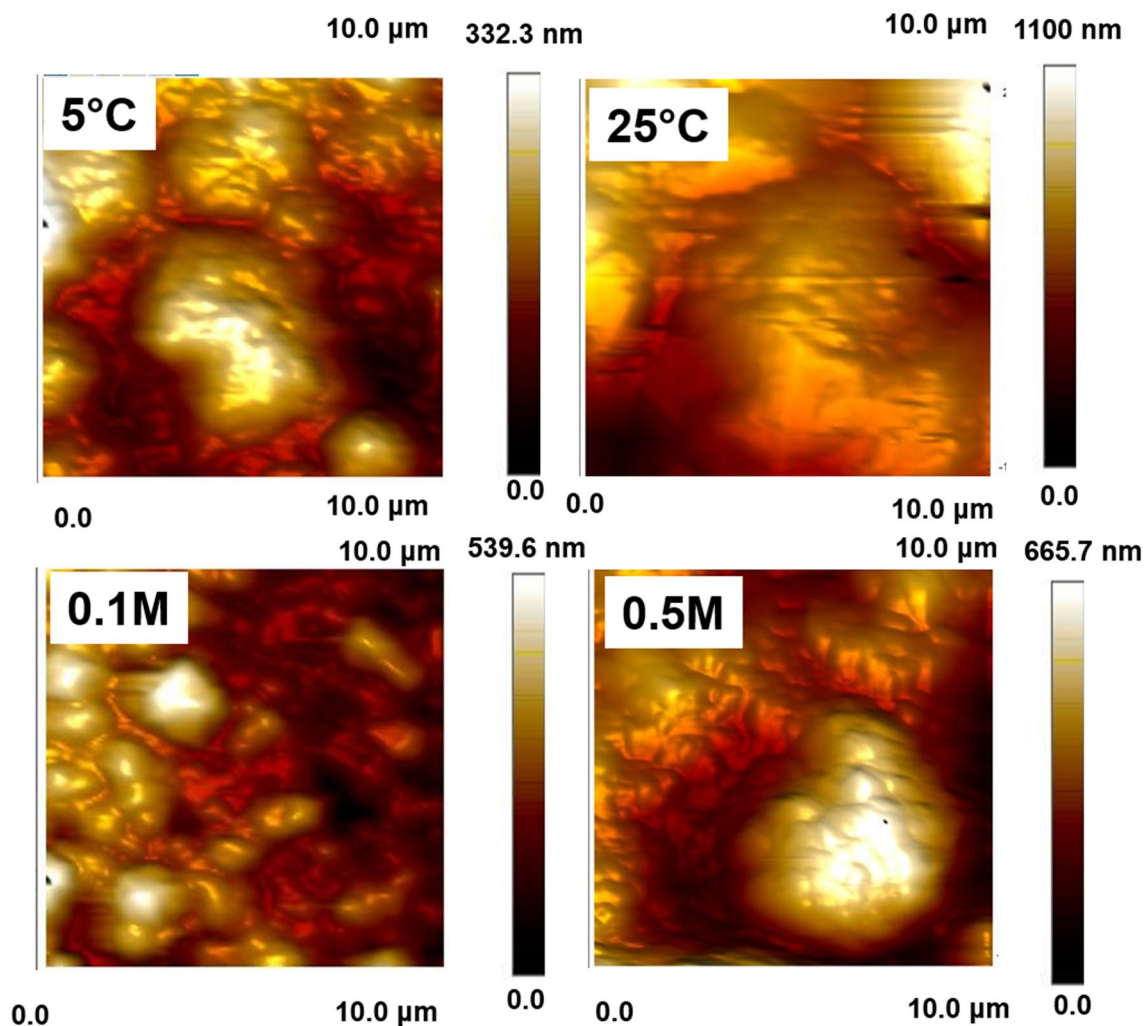


Fig. 6 AFM image for copper films deposited at 5 and 25 °C (at concentrations of 0.25 M), 0.1 M (25 °C), and 0.5 (25 °C)

Acknowledgments The authors express their gratitude for the financial support provided by National Institute of Technology (NIT) to carry out the research work.

Author Contribution SP: Experimentation, conceptualization and preparation of the initial draft, SD: Data curation and Review of the first draft, AM: Supervision, Review and Fund acquisition

Declarations

Conflict of interest There is no conflict to declare.

References

- Milchev A, Stoychev D, Lazarov V, Papoutsis A, and Kokkinidis G, *J. Cryst. Growth* **226** (2001) 138.
- Vazquez-Arenas J, Cruz R, and Mendozahuizar L H, *Electrochim. Acta* **52** (2006) 892.
- Mallik A, and Ray B C, *Thin Solid Films* **517** (2009) 6612.
- Gamburg Y D, *Russ. J. Electrochem.* **52** (2016) 1090.
- Mallik A, and Ray B C, *Surf. Eng.* **27** (2011) 551.
- Grujicic D, and Pesic B, *Electrochim. Acta* **50** (2005) 4426.
- Grujicic D, and Pesic B, *Electrochim. Acta* **47** (2002) 2901.
- Detavernier C, Rossnagel S, Noyan C, Guha S, and Lavoie C, *J. Appl. Phys.* **94** (2003) 2874.
- Ghodbane O, Roué L, and Bélanger D, *Electrochim. Acta* **52** (2007) 5843.
- Majidi M R, Asadpour-Zeynali K, and Hafezi B, *Electrochim. Acta* **54** (2009) 1119.
- Chung C K, Chang W T, Chen C F, and Liao M W, *Mater. Lett.* **65** (2011) 416.
- Ramírez C, Arce E M, Romero-Romo M, and Palomar-Pardave M, *Solid State Ion.* **169** (2004) 81.
- Pasquale M A, Gassa L M, and Arvia A J, *Electrochim. Acta* **53** (2008) 5891.
- Cheng X, Li G, Kneer E A, Vermeire B, and Jeon S, *J. Electrochem. Soc.* **145** (1998) 352.
- Fabricius G, and Sundholm G, *J. Appl. Electrochem.* **14** (1984) 797.
- Brown O R, and Thirsk H R, *Electrochim. Acta* **10** (1965) 383.
- Chassaing E, and Wiart R, *Electrochim. Acta* **29** (1984) 649.

18. Bagotsky V S, *Fundamentals of Electrochemistry*, Wiley, New York (2005).
19. Kang J, Wen J, Jayaram S H, Yu A, and Wang X, *Electrochim. Acta* **115** (2014) 587.

Publisher's Note Springer Nature remains neutral with regard to jurisdictional claims in published maps and institutional affiliations.

Springer Nature or its licensor (e.g. a society or other partner) holds exclusive rights to this article under a publishing agreement with the author(s) or other rightsholder(s); author self-archiving of the accepted manuscript version of this article is solely governed by the terms of such publishing agreement and applicable law.